

the chronic phase is controversial. The undesirable side effects of both drugs are a major drawback in their use, frequently forcing the physician to stop the treatment [3]. In the absence of effective vaccines, chemotherapy plays a critical role in the control of these diseases [4]. The development of safer and more efficient therapeutic anti-*T. cruzi* drugs continues to be a major goal in trypanocidal chemotherapy.

Alkaloids containing a quinazoline nucleus constitute an important group of natural products displaying a wide variety of biological and pharmacological activities. To date, quinazoline, quinazolinone and their derivative compounds have been found to display a diverse set of interesting biological properties such as anticonvulsant [5], antineoplastic [6], antimicrobial [7], antihistamines [8], anti-inflammatory [9] and antimalarial agents [10], as well as cathepsin and monoamino oxidase enzyme inhibitors [11]. Hence, these compounds have gained a great interest in the pharmaceutical chemistry field [12-14]. In this study, we report the synthesis, identification and pharmacological assessment of a new family of heterocyclic compounds derived from quinazolinone and quinazoline with trypanocidal properties.

2. MATERIALS AND METHODS

Melting points (uncorrected) were determined in a capillary tube with an Electrothermal 9100 SERIES-Digital apparatus. The microwave-assisted synthesis of compounds was carried out in Monowave 300 Anton Paar. Reactions were monitored by thin-layer chromatography (TLC) on silica gel plates (F245 Merck) and the products were visualized under ultraviolet light (254 and 365 nm). Column chromatography was carried out employing Merck silica gel (Kieselgel 60, 63-200 μm). ^1H - and ^{13}C -NMR spectra were determined in DMSO- d_6 and CDCl_3 solutions in a Bruker 300 MHz and Bruker Biospin 600 MHz AVIII600 spectrometers at room temperature with tetramethylsilane as internal standard. Chemical shifts (δ) were reported in ppm and coupling constants (J) in Hertz. The mass spectrometer utilized was a Xevo G2S QTOF (Waters Corporation, Manchester, UK) with an electrospray ionization (ESI) source. The purity ($\geq 95\%$) of all final synthesized compounds was determined by reverse phase HPLC using a Waters 2487 dual λ absorbance detector with a Waters 1525 binary pump and a $5\mu\text{m}$ pd C18(2) and 250×4.6 mm Phenomenex Luna column. Samples were run at 1mL min^{-1} using gradient mixtures of 5-100% of water with 0.1% trifluoroacetic acid (TFA) (A) and acetonitrile:water (10:1) with 0.1% TFA (B) for 22 min followed by 3 min at 100% B. UV spectra were recorded with a Shimadzu 3600 UV/vis/NIR spectrophotometer.

2.1. Synthesis

The general procedures for the synthesis of all compounds and the spectroscopic and HR-MS (ESI) data of the representative compounds are given in this section. Spectroscopic characterization and physical data of all the compounds are found in the supplementary material.

2.1.1. General Procedure for the Synthesis of Compounds 4a-c

A mixture of the corresponding ethyl anthranilate (1) (0.77 g, 5.0 mmol) and phenyl isocyanate (2) (0.55g, 5.0

mmol) was dissolved in dry dioxane (10 ml) and refluxed until no starting material remained (3-8 h), as assessed by TLC. Amberlyst-15 resin was added and heated overnight until reaction was completed and a white solid appeared. The reaction mixture was dissolved in hot methanol and the resin was filtered and washed. The organic solvent was removed under reduced pressure and the crude product was purified by recrystallization from ethanol or DMF-isopropanol to obtain pure 4a-c as a white solid.

2.1.1.1. 3-(4-chlorophenyl)-6,7-dimethoxyquinazoline-2,4(1H,3H)-dione (4c)

Time reaction: 8 h. Yield: 1.33 g, 81 % (DMF-isopropanol). Mp: 304-306°C. ^1H NMR (600 MHz, DMSO- d_6) δ : 11.36 (s, 1H), 7.54 (d, $J = 8.6$ Hz, 2H, Ar), 7.35 (d, $J = 8.6$ Hz, 2H), 7.28 (s, 1H), 6.73 (s, 1H), 3.86 (s, 3H), 3.79 (s, 3H). ^{13}C NMR (151 MHz, DMSO- d_6) δ : 162.0, 155.7, 150.5, 145.7, 136.0, 135.3, 133.3, 131.6, 129.2, 108.4, 106.5, 98.1, 56.4. HR-MS (ESI) calcd for $\text{C}_{16}\text{H}_{13}\text{ClN}_2\text{O}_4$ $[\text{M}+1]^+$ m/z : 333.0564, found: 333.0559.

2.1.2. General Procedure for Synthesis of Compounds 4d-e

2.0 mmol of isatoic anhydride (0.32 g) and 4.0 mmol of benzylamine or 2-chlorobenzylamine were heated at 160°C until complete disappearance of the starting material by TLC (0.5 h). The solid was allowed to cool and suspended in 95% EtOH. The suspension was filtered and the white solid was purified by recrystallization from EtOH: H_2O to give compounds 4d-e.

2.1.2.1. 3-(2-chlorobenzyl)quinazoline-2,4(1H,3H)-dione (4e)

Yield: 0.40 g, 70%. Mp: 211-212°C. ^1H NMR (300 MHz, CDCl_3) δ : 10.43 (s, 1H), 8.00 (dd, $J = 7.4$, 2.0 Hz, 1H), 7.52-7.34 (m, 3H), 7.27 (td, $J = 7.5$, 2.0 Hz, 1H), 7.00-7.19 (m, 3H), 6.01 (s, 2H). ^{13}C NMR (75 MHz, CDCl_3) δ : 161.6, 150.5, 139.2, 135.5, 135.1, 134.9, 130.33, 129.9, 129.8, 127.3, 126.9, 122.2, 115.1, 113.8, 45.0. HR-MS (ESI) calcd. for $\text{C}_{15}\text{H}_{11}\text{ClN}_2\text{O}_2$ $[\text{M}+1]^+$ m/z : 287.0509, found: 287.0505.

2.1.3 General Procedure for the Synthesis of Compounds 5a-c

Phenacyl bromide (0.12 g, 0.6 mmol) in acetone (1.0 mL) was added to a solution of the corresponding compounds 4a-c (0.5 mmol) and potassium carbonate (0.34 g, 2.5 mmol) in acetone (20 mL). The reaction mixture was stirred and refluxed in acetone for 3-5 h. The solvent was evaporated under reduced pressure. The residue was treated with water, acidified with a saturated aqueous NH_4Cl solution, and extracted with DCM (30 mL \times 3). The combined organic layer was washed with brine (30 mL), dried over anhydrous MgSO_4 , filtered, and evaporated under reduced pressure. The solid was recrystallized from EtOH to obtain compounds 5a-c.

2.1.3.1. 1-(2-oxo-2-phenylethyl)-3-phenylquinazoline-2,4(1H,3H)-dione (5a)

Reaction time: 3 h. White solid (ethanol). Yield: 0.14 g, 80%. Mp: 224-225°C. ^1H NMR (600 MHz, CDCl_3) δ : 8.29 (dd, $J = 7.9$, 1.6 Hz, 1H), 8.07 – 8.04 (m, 2H), 7.70 – 7.64 (m, 1H), 7.62 (ddd, $J = 8.7$, 7.3, 1.7 Hz, 1H), 7.53 (dtd, $J =$

19.4, 7.0, 6.6, 1.6 Hz, 4H), 7.47 – 7.42 (m, 1H), 7.34– 7.30 (m, 2H), 7.30–7.25 (m, 1H), 6.91 (d, $J = 8.4$ Hz, 1H), 5.64 (s, 2H). ^{13}C NMR (151 MHz, CDCl_3) δ : 191.9, 161.8, 151.3, 140.3, 135.4, 135.4, 134.54, 134.34, 129.6, 129.4, 129.1, 128.8, 128.4, 128.1, 123.3, 116.1, 113.6, 49.8. HR-MS (ESI) calcd. for $\text{C}_{22}\text{H}_{16}\text{N}_2\text{O}_3$ $[\text{M}+1]^+$ m/z : 356,1161, found: 356,1158.

2.1.3.2. 1-(2-oxo-2-phenylethyl)-3-(4-chlorophenyl) quinazoline-2,4(1H,3H)-dione (5b)

Reaction time: 3 h. White solid (ethanol). Yield: 0.13 g, 66%. Mp: 223–225°C. ^1H NMR (600 MHz, CDCl_3) δ : 8.22 (dd, $J = 7.9, 1.6$ Hz, 1H), 8.02 – 7.96 (m, 2H), 7.64 – 7.59 (m, 1H), 7.56 (ddd, $J = 8.7, 7.2, 1.7$ Hz, 1H), 7.49 (t, $J = 7.8$ Hz, 2H), 7.44 – 7.38 (m, 2H), 7.26 – 7.17 (m, 3H), 6.85 (d, $J = 8.4$ Hz, 1H), 5.57 (s, 2H). ^{13}C NMR (151 MHz, CDCl_3) δ : 191.7, 161.6, 151.0, 140.2, 135.6, 134.7, 134.4, 133.8, 129.90, 129.6, 129.1, 128.1, 123.4, 115.9, 113.6, 49.8. HR-MS (ESI) calcd. for $\text{C}_{22}\text{H}_{15}\text{ClN}_2\text{O}_3$ $[\text{M}+1]^+$ m/z : 391.0771, found: 391.0769.

2.1.4. General Procedure for the Synthesis of Compounds 9a-h

A stirred mixture of isatoic anhydride (0.33 g, 2.0 mmol), the corresponding aldehyde (2.0 mmol) and amine (2.0 mmol), and Amberlyst-15 resin (0.01 g), in EtOH- H_2O (7:1 (v/v), 8 mL), was heated under reflux conditions for 2 h. After reaction completion, the mixture was cooled to room temperature, and hot EtOH (25 mL) was added. The catalyst was filtered off, washed with hot EtOH, and dried. The product was recrystallized from EtOH.

2.1.4.1. 4-(4-oxo-2-phenyl-1,2-dihydroquinazolin-3(4H)-yl)benzoic Acid (9a)

Yield: 0.56 g, 89%. Mp: 238–240°C. Mp Lit [15]: 219–220°C. ^1H NMR (600 MHz, $\text{DMSO}-d_6$) δ : 10.28 (s, 1H), 7.90 (d, $J = 8.5$ Hz, 2H), 7.83 – 7.79 (m, 1H), 7.73 (d, $J = 7.7$ Hz, 1H), 7.49 – 7.34 (m, 4H), 7.34 – 7.19 (m, 4H), 6.79 (d, $J = 8.1$ Hz, 1H), 6.72 (t, $J = 7.5$ Hz, 1H), 6.41 (d, $J = 2.5$ Hz, 1H). ^{13}C NMR (151 MHz, $\text{DMSO}-d_6$) δ : 172.0, 167.6, 151.8, 149.9, 145.6, 139.3, 135.0, 134.9, 133.7, 133.6, 132.9, 131.8, 130.5, 122.9, 120.5, 120.3, 77.1. HR-MS (ESI) calcd for $\text{C}_{21}\text{H}_{16}\text{N}_2\text{O}_3$ $[\text{M}+1]^+$ m/z : 345.1161, found: 345.1160.

2.1.4.1. 2-(benzo[d][1,3]dioxol-5-yl)-3-phenyl-2,3-dihydroquinazolin-4(1H)-one (9b)

Yield: 0.59 g, 87%. Mp: 222–224°C. ^1H NMR (600 MHz, $\text{DMSO}-d_6$) δ : 7.72 (d, $J = 7.5$ Hz, 1H), 7.54 (d, $J = 2.1$ Hz, 1H), 7.33 (t, $J = 7.8$ Hz, 2H), 7.31 – 7.23 (m, 3H), 7.19 (t, $J = 7.3$ Hz, 1H), 6.93 (s, 1H), 6.80 (s, 2H), 6.79 – 6.69 (m, 2H), 6.20 (d, $J = 2.4$ Hz, 1H), 5.96 (d, $J = 5.3$ Hz, 2H). ^{13}C NMR (151 MHz, $\text{DMSO}-d_6$) δ : 162.3, 147.3, 147.2, 146.5, 140.7, 134.6, 133.8, 128.6, 128.0, 127.9, 126.2, 126.0, 120.3, 117.6, 115.3, 114.8, 107.8, 106.9, 106.8, 101.2, 72.4. HR-MS (ESI) calcd. For $\text{C}_{21}\text{H}_{16}\text{N}_2\text{O}_3$ $[\text{M}+1]^+$ m/z : 345.1161, found: 345.1159.

2.1.4.2. 3-(4-methyl-3-nitrophenyl)-2-phenyl-2,3-dihydroquinazolin-4(1H)-one (9h)

Yield: 0.48g, 68%. Mp: 175–178°C. ^1H NMR (600 MHz, $\text{DMSO}-d_6$) δ : 7.92 (d, $J = 2.2$ Hz, 1H), 7.75 – 7.69 (m, 2H),

7.53 (dd, $J = 8.3, 2.1$ Hz, 1H), 7.44 (d, $J = 8.3$ Hz, 1H), 7.39 (d, $J = 7.6$ Hz, 2H), 7.33 – 7.23 (m, 4H), 6.79 (d, $J = 8.2$ Hz, 1H), 6.76 – 6.70 (m, 1H), 6.44 (d, $J = 2.6$ Hz, 1H), 2.46 (s, 3H). ^{13}C NMR (151 MHz, $\text{DMSO}-d_6$) δ : 163.0, 149.0, 147.3, 140.4, 139.6, 134.6, 133.2, 131.4, 130.7, 129.0, 128.9, 128.5, 127.2, 122.3, 118.2, 115.4, 115.2, 72.7, 19.6. HR-MS (ESI) calcd. for $\text{C}_{21}\text{H}_{17}\text{N}_3\text{O}_3$ $[\text{M}+1]^+$ m/z : 360.1270, found: 360.1276.

2.1.5. General Procedure for the Synthesis of Compounds 13a-r

A solution of NH_4OH (28 % w/w, 0.7mL) was added dropwise at room temperature to a suspension of isatoic anhydride (1.0 g, 6.0 mmol) in a mixture of acetonitrile: water (3:1 (v/v), 20 mL). The reaction mixture was stirred for 1h and extracted with EtOAc (3 x 15 mL). The organic layer was dried over anhydrous Na_2SO_4 and concentrated *in vacuo* to yield compound **10** which was used directly without further purification. Sodium hydrogen sulfite (0.4 g, 3.8 mmol) was added to a solution of 2-aminobenzamide (**10**) (0.5 g, 3.8 mmol) and the corresponding aldehyde (3.8 mmol) in DMAC (10 mL). The mixture was heated at 150 °C for 2h and poured onto ice water and dried *in vacuo*. Compounds **11a-c** were purified by recrystallization from EtOH or by column chromatography employing hexane:EtOAc (70:30) as mobile phase.

Compounds **11a-c** (4.6 mmol) were dissolved in phosphoryl chloride (5.0 mL, 53.6 mmol) and the mixture was stirred and heated at 115 °C for 16 h. The solvent was then evaporated and then co-evaporated with toluene. The residue was dissolved with EtOAc and 10% NaOH was added dropwise. The organic layer was sequentially washed with water and brine (3 x 15 mL), dried over anhydrous Na_2SO_4 and concentrated *in vacuo*. The crude product was purified by column chromatography employing hexane:EtOAc, (70:30) as mobile phase to give compounds **12a-c**. Finally, compounds **13a-r** were obtained through either conventional heating or microwave heating by following the procedure described below.

Conventional heating: DIPEA (0.75 mmol) in THF (1 mL) was added to a pressure vial containing the mixture of the desired monosubstituted quinazoline (**12a-c**) (0.25 mmol) and the required amine (0.25 mmol). The mixture was heated under reflux conditions until the TLC analysis indicated the complete conversion of the starting material into the disubstituted quinazoline. The solution was allowed to cool to room temperature, quenched with saturated NaHCO_3 solution or water, and partitioned with EtOAc (3 x 15 mL). The organic layer was sequentially washed with brine (3 x 15 mL), dried over anhydrous Na_2SO_4 and concentrated *in vacuo*. The residue was purified by column chromatography (SiO_2 , Hexane/EtOAc, gradient: 100:0 to 60:40) to afford the desired compounds **13a-r**.

Microwave heating: a microwave tube was loaded with the corresponding monosubstituted quinazoline (**12a-c**) (0.25 mmol), the corresponding amine (0.25 mmol) and isopropanol (1 mL). The mixture was heated at 80 °C for 5 min. The resulting suspension was then diluted with EtOAc and washed with water and brine. The subsequent drying over Na_2SO_4 and evaporation of the solvent yielded a dark solid

that was purified by column chromatography (SiO₂, Hexane/EtOAc, gradient: 100:0 to 60:40) to afford the desired compounds **13a-r**.

2.1.5.1. 2-(benzo[d][1,3]dioxol-5-yl)-N-(2-chlorobenzyl)quinazolin-4-amine (13f)

Conventional heating: Yield: 0.07 g, 72%. Mp: 215–217°C. ¹H NMR (500 MHz, DMSO-*d*₆) δ: 8.92 (t, *J* = 5.7 Hz, 1H), 8.35 (d, *J* = 8.2 Hz, 1H), 8.01 (dd, *J* = 8.2, 1.2 Hz, 1H), 7.86 – 7.70 (m, 3H), 7.55 – 7.47 (m, 3H), 7.31 – 7.24 (m, 2H), 6.98 (d, *J* = 8.2 Hz, 1H), 6.08 (s, 2H), 4.97 (d, *J* = 5.6 Hz, 2H). ¹³C NMR (126 MHz, DMSO-*d*₆) δ: 167.0, 159.9, 159.1, 150.4, 149.5, 137.1, 133.3, 133.27, 129.6, 129.1, 129.0, 128.2, 127.7, 125.7, 123.2, 122.9, 114.1, 108.4, 108.1, 101.8, 42.1. HR-MS (ESI) calcd. for C₂₂H₁₆ClN₃O₂ [M+1]⁺ *m/z*: 390.0897, found: 390.0898.

2.1.5.2. N-benzyl-2-(4-methoxyphenyl)quinazolin-4-amine (13p)

Microwave heating: Yield 0.07g, 85%. Mp: 148–150°C. ¹H NMR (600 MHz, CDCl₃) δ: 8.59 – 8.48 (m, 2H), 7.91 (d, *J* = 8.5 Hz, 1H), 7.72 (ddd, *J* = 8.3, 6.9, 1.3 Hz, 1H), 7.67 (dd, *J* = 8.1, 1.3 Hz, 1H), 7.50 – 7.46 (m, 2H), 7.39 (tt, *J* = 6.8, 1.0 Hz, 3H), 7.35 – 7.31 (m, 1H), 7.02 – 6.98 (m, 2H), 5.90 (s, 1H), 5.02 (d, *J* = 5.4 Hz, 2H), 3.89 (s, 3H). ¹³C NMR (151 MHz, CDCl₃) δ: 160.4, 159.4, 150.9, 138.9, 132.8, 131.7, 130.2, 129.0, 128.3, 127.8, 125.2, 120.6, 113.8, 113.5, 55.5, 45.5. HR-MS (ESI) calcd for C₂₂H₁₉N₃O [M+H]⁺ *m/z*: 342.1140, found 342.1191

2.1.5.3. N-(4-methoxyphenyl)-2-phenylquinazolin-4-amine (13q)

Microwave heating: Yield: 0.07, 88%. Mp: 150–152°C. ¹H NMR (600 MHz, DMSO-*d*₆) δ: 11.58 (s, 1H), 8.90 (d, *J* = 8.3 Hz, 1H), 8.40 – 8.32 (m, 3H), 8.08 (ddd, *J* = 8.3, 7.0, 1.2 Hz, 1H), 7.82 (t, *J* = 7.7 Hz, 1H), 7.79 – 7.74 (m, 2H), 7.74 – 7.68 (m, 1H), 7.65 (t, *J* = 7.7 Hz, 2H), 7.14 – 7.08 (m, 2H), 3.84 (s, 3H). ¹³C NMR (151 MHz, DMSO-*d*₆) δ: 159.2, 158.0, 157.7, 136.2, 133.7, 130.1, 129.6, 129.4, 128.4, 126.4, 124.9, 114.4, 113.1, 55.8. HR-MS (ESI) calcd. for C₂₁H₁₇N₃O, [M+H]⁺ *m/z*: 328.1449, found: 328.1450.

2.1.5.4. N-(4-chlorobenzyl)-2-phenylquinazolin-4-amine (13r)

Conventional heating: Yield: 0.04 g, 41%. *Microwave heating:* Yield: 0.07 g, 82%. Mp: 174–182°C. ¹H NMR (300 MHz, DMSO-*d*₆) δ: 8.96 (t, *J* = 5.5 Hz, 1H), 8.42 (dd, *J* = 6.6, 3.0 Hz, 2H), 8.30 (d, *J* = 8.3 Hz, 1H), 7.79 (d, *J* = 3.6 Hz, 2H), 7.57 – 7.33 (m, 8H), 4.90 (d, *J* = 5.7 Hz, 2H). ¹³C NMR (75 MHz, DMSO-*d*₆) δ: 160.0, 159.6, 150.4, 139.4, 138.9, 133.2, 131.6, 130.4, 129.7, 128.7, 128.3, 125.9, 123.1, 114.2, 43.7. HR-MS (ESI) calcd. for, C₂₁H₁₆ClN₃, [M+H]⁺ *m/z*: 328.1449, found: 328.1450.

2.2. Biology

2.2.1. Parasites and Mammalian Cells

T. cruzi epimastigotes (Tulahuen strain, Tul 2 stock) were grown at 28 °C in a liquid culture medium containing 3.3% brain-heart infusion (Difco); 0.3% tryptose (Difco); 0.3% disodium phosphate; 0.04% potassium chloride; 0.03%

dextrose and 20 g mL⁻¹ hemin. After sterilization, penicillin (100 IU mL⁻¹), streptomycin (100 μg mL⁻¹) and 10% v/v heat-inactivated fetal calf serum were added. *T. cruzi* bloodstream trypomastigotes were obtained from infected CF1 mice by cardiac puncture, at the peak of parasitemia on day 15 post-infection. Trypomastigotes were routinely maintained by infecting 21-day-old CF1 mice (weighing 23.8 ± 2.6 g). Inbred CF1 male mice were nursed at the animal facility in Facultad de Medicina, Universidad de Buenos Aires. Animals were handled in accordance with guidelines established by the Animal Care and Use Committee of the Argentine Association of Specialists in Laboratory Animals (AADEALC). The Vero cell line was cultured in RPMI medium, supplemented with 10% FBS, 100 U mL⁻¹ penicillin and 0.1 mg mL⁻¹ streptomycin.

2.2.2. In vitro Trypanocidal Activity Assay

To evaluate the growth inhibition of *T. cruzi* epimastigotes, parasites were inoculated into fresh culture medium to reach an initial concentration of 1.5–2.5 × 10⁶ cells mL⁻¹. Parasites were then cultured for 4 days in the presence of different concentrations (2.50–15 μM) of the compounds to be tested or Bnz (as reference trypanocidal drug). The inhibition of parasite growth was evaluated and compared to control cultures without compounds. The parasites growth was monitored by counting the number of parasites per mL of culture using a Neubauer chamber and expressed as cell density (CD). For the count, only motile parasites were taken into account. The percentage of inhibition (%I) was calculated as: %I = {1 - [(CD_{4t} - CD_{0t}) / (CD_{4c} - CD_{0c})]} × 100, where CD_{4t} is the CD of treated cultures measured on day 4; CD_{0t} is the CD of treated cultures measured immediately after adding the drug (day 0); CD_{4c} is the CD of untreated cultures (control) measured on day 4; and CD_{0c} is the CD of untreated cultures measured on day 0.

The trypanocidal effects of different compounds and Bnz were also tested on bloodstream trypomastigotes according to a standard WHO protocol with minor modifications [16–17]. The IC₅₀ epi and IC₅₀ trypo (50% inhibitory concentration on epimastigotes and trypomastigotes, respectively), was estimated by non-linear regression analysis (sigmoidal curve) from the %I values and the decimal logarithm (log) of drug concentration.

2.2.3. Cytotoxicity Assay

To evaluate the cytotoxic activity, Vero cells (1.5 × 10⁵ cell/mL) were seeded in a 24-well plate and after 24 h of incubation, different concentrations of each synthesized compound (12 - 120 μM) or Bnz (3 - 300 μM) were added. After 48 h of incubation, cells were washed with PBS and 3-(4,5-dimethylthiazol-2-yl)-2,5-diphenyltetrazolium bromide (MTT) was added at a final concentration of 0.5 mg mL⁻¹. Plates were incubated for 1h at 37 °C, the purple precipitate was then dissolved in 0.5 mL DMSO and read on a plate reader (Spectra CountTM BS 10001) at 570 nm. Treated cells were compared with the untreated control, which were taken as 100% viability. The CC₅₀ (50% cytotoxic concentration) was calculated by non-linear regression analysis (sigmoidal curve) from the percentage of viable cells and the decimal logarithm (log) of drug concentration.

Results are representative of three to four separate experiments, performed in duplicate or triplicate. Data are expressed as means \pm standard errors of the mean (SEMs). Non-linear regression analyses were done using the Sigma Plot 12 software.

2.3. Computational Chemistry

2.3.1. ADME Prediction

ADME predictions were carried out for the lead candidates in order to check the pharmacological activity using the QikProp 2.1 module [18].

2.3.2. Quantitative-structure Activity Relationship

Molecular structures were drawn in MarvinSketch 17.3.13.0. The resulting 2D geometry was transferred into the PaDel-Descriptor program package in order to obtain 1444 descriptors which included constitutional, topological, geometrical, 2D autocorrelation, and electrotopological classes [19]. Those molecular descriptors with zero variances or more than 90% of zero values were deleted. To generate two-class models, and based on their activity, the data set was divided into active and inactive compounds. Compounds with anti-epimastigote activity $IC_{50} < 15 \mu M$ were considered active and compounds with $IC_{50} > 15 \mu M$ were considered inactive. For the trypanomastigote activity, compounds with $IC_{50} < 120 \mu M$ were considered active and compounds with $IC_{50} > 120 \mu M$ were considered inactive. At this point, a set of compounds was selected employing a stratified sampling as a prediction set (PS), and these compounds were not used anywhere in the model development but for validation. The remaining compounds comprised the training set (TS) [20]. The highly correlated descriptors, multicollinearity and useless descriptors were eliminated. In this work, for the classification via regression, we employed the M5' algorithm as implemented in Weka [21-22].

The Molegro Virtual Docker 4.1 software was used to manipulate the data to generate several classic QSAR multiple linear regression (MLR) models [23] using the structures displaying quantitative activity on epimastigotes and trypanomastigotes (pIC_{50}). The descriptors are ranked according to the Pearson correlation coefficient between each descriptor and the target variable. The quality/performance of each feature selection solution is evaluated using the criterion training set that uses a Forward Selection method to evaluate model performance, balancing model accuracy (Mean Squared Error, MSE) and model complexity (number of descriptors used in the model) [24]. Finally, the generated QSAR model is used against itself using a Leave-One-Out cross-validation (LOOCV) strategy [25]. In this work, we extended the classic MLR methodology with a back-propagation neural network analysis (BNN) approach (utilizing LOOCV). The artificial neural network analysis (ANN) is one of the most widely used methods for developing non-linear models. More details about ANN theory have been described elsewhere [26]. The BNN is a gradient descent on the error surface, the weights of the connections between neurons being adjusted in order to decrease the root mean squared error between calculated and expected values for all molecules in the training set.

2.4. Physicochemical Properties

2.4.1 Shake-flask Method for drug Solubility Testing

The shake-flask method was used as a reference assay [27]. Representative compounds (**5a**, **5b**, **9b**, **9h**, **13f** and **13p**) (1.0 mg) were weighed into 2.5 mL glass vials, and the medium (buffer solution at pH 7.4; 6.5 or 2.0) was added. The vial contents were mixed at 600 rpm at 37 °C. After 48 h, the sample was filtered (0.2 μM , Sterile Acrodisc® 13, GelmanScience) before UV analysis. Calibration curves were obtained from a series of compounds over a wide concentration range and constructed by plotting absorbance of the compounds against the concentration. All compounds were tested in triplicate.

3.4.2 PBS Stability

A 100 μM solution of compounds (**5a**, **5b**, **9b**, **9h**, **13f**, **13p**) was prepared in phosphate buffered saline (PBS), pH 7.4, from a 25 μM stock solution in DMSO. The storage vials were then incubated at 37 °C and shaken at 100 rpm for 48 h. Samples were taken at 0 min, 30 min, 1 h, 2 h, 4 h, 8 h, 24 h, and 48h. The samples were subjected to vortex mixing for 1 min and then centrifugation at 4°C for 15 min at 14,000 rpm. The clear supernatants were analyzed by UV-vis. The values represent the mean of three independent experiments. Percentage stability was determined using the chromatographic peak area. All the samples were prepared in triplicate.

3. RESULTS AND DISCUSSIONS:

3.1. Chemistry

Quinazolines and quinazolinones are compounds featured by the presence of fused heterocycles which are of considerable interest because of the wide range of biological properties they display. Taking into account such characteristics, our goal was to synthesize a new series of quinazolinone and quinazoline derivatives having anti-chagasic activity (Fig. 2). The desired compounds were obtained in multistep reactions, as shown in Scheme 1-4.

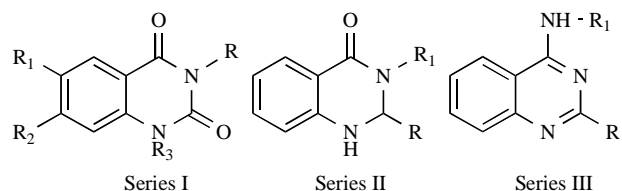
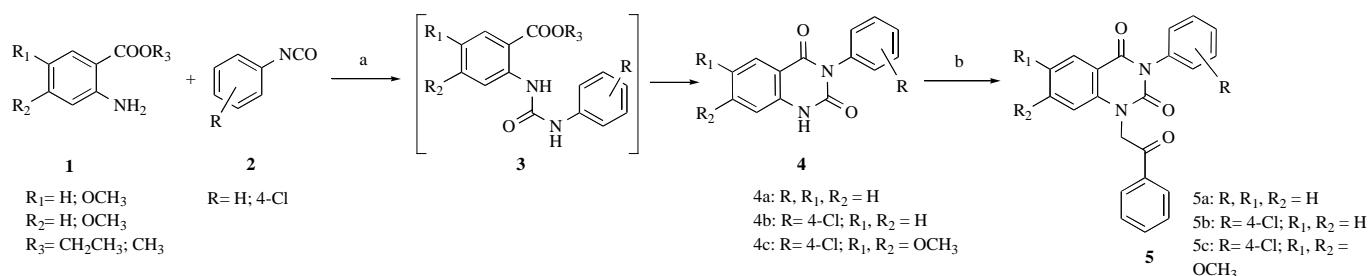
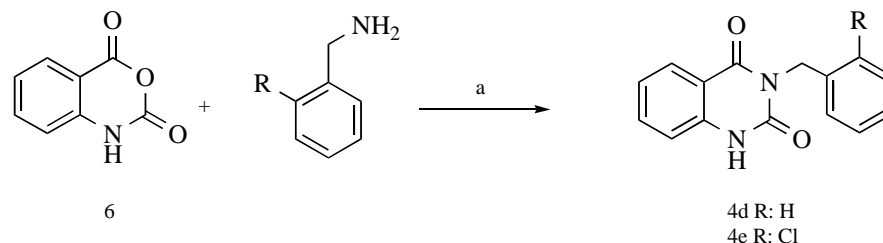


Fig. (2). Structure of the series of quinazolinone and quinazoline derivatives synthesized.

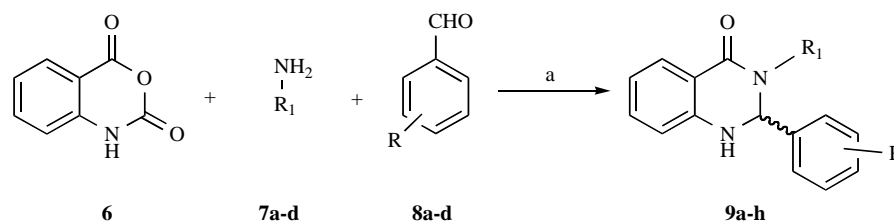
The most common methods of synthesis of quinazolinodiones (*Series I*) involve the reaction between methyl anthranilates and isocyanates with base catalysis [28], and between isatoic anhydride and amines and isocyanates and subsequent reaction with diethyl carbonate, [29] triphosgene [30] or trichloroacetyl chloride [31]. In all cases the synthesis consists of more than one reaction step, drastic conditions and the use of highly toxic reagents. Herein, we report the synthesis of 3-arylquinazoline-2,4(1*H*,3*H*)-diones in a one-pot process that involves the reaction between ethyl 2-aminobenzoates (**1**) and arylisocyanates (**2**), using macro-



Scheme 1. Synthesis of compounds **4a-c** and **5a-c**. Reagents and conditions: (a) Amberlyst 15, dioxane (b) phenacyl bromide, K_2CO_3 , acetone.



Scheme 2. Synthesis of compounds **4d-e**. Conditions: (a) 160°C , 30 min.



Scheme 3. Synthesis of compounds **9a-h**. Reagents and conditions: (a) Amberlyst-15, EtOH:water (7:1), reflux, 2h.

reticular resins such as Amberlyst 15 acid catalyst in refluxing dry dioxane. First, an intermediate compound, 2-(3-arylethylureido)-ethylbenzoate (**3**) is formed, and without isolating provides the corresponding quinazolinone (**4a-c**) by a cyclization reaction with the subsequent loss of ethanol. The corresponding salts of these compounds were generated by the reaction with potassium carbonate in acetone and subsequently treated with phenacyl bromide to obtain the N-1 alkylated derivatives (**5a-c**) (Scheme 1).

Compounds **4d-e** were synthesized from isatoic anhydride and benzylamine or 2-chlorobenzylamine by heating to reflux without solvent as shown in Scheme 2.

Different strategies for the synthesis of quinazolinones (Series II, Fig. 2) have been widely described in the literature [15, 32-34]. In this work, we report an efficient procedure for the synthesis of disubstituted quinazolinones via a one-pot condensation of isatoic anhydride, aldehyde and amine in the presence of Amberlyst-15 under classical heating conditions (Scheme 3).

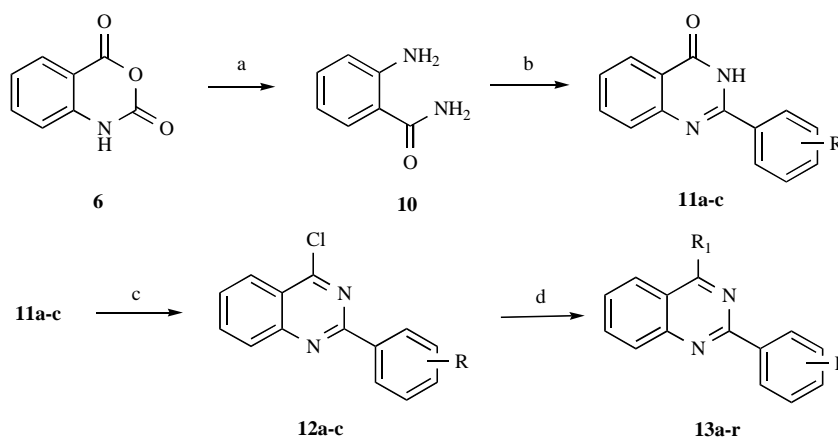
In order to optimize the reaction conditions, we carried out the reaction with isatoic anhydride (2.0 mmol), aniline (2.0 mmol) and benzaldehyde (2.0 mmol) as a model reaction in the presence of different amounts of solvents and catalyst under reflux (Table 1). The reaction was carried out in pure water, EtOH or EtOH- H_2O . After several attempts, the results showed that the EtOH- H_2O (7:1) system was the best choice.

Table 1. Optimization of solvent and catalyst conditions for the synthesis of **9a**.

Catalyst	Solvent (mL)	Yield, %
Amberlyst-15 (0.0g)	EtOH	12
Amberlyst-15 (0.005g)	EtOH	35
Amberlyst-15 (0.010g)	EtOH	41
Amberlyst-15 (0.010g)	H_2O	15
Amberlyst-15 (0.010g)	EtOH: H_2O (9:1)	55
Amberlyst-15 (0.010g)	EtOH: H_2O (8:1)	77
Amberlyst-15 (0.010g)	EtOH: H_2O (7:1)	89
Amberlyst-15 (0.010g)	EtOH: H_2O (6:1)	66

The general procedure employed for the synthesis of members of the 2,4-disubstituted quinazolinone derivatives series (Series III, Fig. 2) (13a-r) is shown in Scheme 4.

2-Aminobenzamide (**10**), employed as a starting point, was prepared using a standard methodology [35]. Compound **10** reacted with the corresponding aldehyde in dimethylacetamide (DMAC) in the presence of NaHSO_3 at 150°C . The thermal cyclodehydration/dehydrogenation afforded the substituted 2-phenyl-4-quinazolines (**11a-c**). Finally, the



Scheme 4. Synthesis of compounds 13a-r. Reagents and conditions: (a) Et₃N, NH₄OH (28 % w/w), H₂O, MeCN, rt, 1 h; (b) aldehyde, NaHSO₃ DMAC, 150°C, 2h. (c) POCl₃, 115°C, 16h; (d) DIPEA, THF, reflux, 24-48 h or microwave irradiation, amine, isopropanol, 80°C, 5 min.

Table 2. *In vitro* anti-trypanosomal activity and cytotoxicity of quinazolin-2(1H)-one derivatives.

Series I							
Cmpd.	R	R ₁	R ₂	R ₃	IC ₅₀ Epi (μM)	IC ₅₀ Trypo (μM)	CC ₅₀ (μM)
4a	Ph	H	H	H	>15	>100	ND
4b	4-ClPh	H	H	H	>15	>100	ND
4c	4-ClPh	CH ₃ O	CH ₃ O	H	>15	>100	>>120
4d	Bz	H	H	H	11.79 ± 0.96	115.55 ± 3.50	117.10 ± 5.80
4e	2-ClBz	H	H	H	11.25 ± 0.25	>>100	>>120
5a	Ph	H	H	PhCOCH ₂	15.89 ± 0.75	48.45 ± 5.65	>>120
5b	4-ClPh	H	H	PhCOCH ₂	12.68 ± 0.42	57.80 ± 6.20	>>120
5c	4-ClPh	CH ₃ O	CH ₃ O	PhCOCH ₂	13.04 ± 0.95	48.50 ± 7.15	186.99 ± 5.70
Bnz	-	-	-	-	5.49 ± 0.49	30.26 ± 2.85	87.25 ± 3.24

desired compounds (**13a-r**) were prepared by S_NAr chemistry from 4-chloro quinazoline (**12a-c**) and the corresponding alkyl or phenyl amines. The reaction was carried out in seal tube under reflux conditions for 24 or 48 h to obtain a good yield. In order to accelerate the chemical reaction, the microwave technique was used employing isopropanol as solvent. The desired compounds were obtained in only 5 min in a very good yield.

3.2. Biological Activity

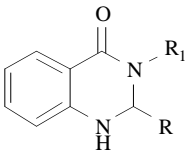
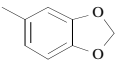
3.2.1. Evaluation of anti-*T. cruzi* Activity

After the structural characterization of the synthesized compounds, the antiparasitic activity against *T. cruzi* epimastigotes and trypomastigotes and cytotoxicity activity on Vero cells were determined. The antiparasitic and cytotoxic activities were expressed in terms of IC₅₀ and CC₅₀ values, respectively. Bnz was used as a reference antiparasitic drug.

The compounds derived from quinazolin-2(1H)-one (*Series I*, 4-5) wherein R₁ is a phenyl or a 4-chlorophenyl with or without substitution on the fused aromatic ring (**4a-c**) were found to be inactive against both epimastigotes and trypomastigotes. However, compounds *N*-1 substituted (**5a-c**) with a phenacyl group showed a slight antiparasitic activity on epimastigotes, whereas on trypomastigotes, the activity was similar to that of Bnz. In addition, the quinazolin-2(1H)-one substituted with a benzyl or a 2-chlorobenzyl in the R₁ position (**4d**, **4e**) showed activity only against the epimastigote form. In this series, compounds **5a** and **5b** were found to be the most active on the trypomastigote stage, which leads us to conclude that the substitution in *N*-1 with the phenacyl group is favorable for the activity against this infective form. Unlike **5c**, compounds **5a** and **5b** did not show any cytotoxicity on Vero cells (Table 2).

Compound **9d** derived from *Series II* showed activity against the epimastigote stage. Compounds **9b** and **9h** had

Table 3. *In vitro* anti-trypansomal activity and cytotoxicity of quinazolinones derivatives.

Series II					
Cmpd.	R	R ₁	IC ₅₀ Epi (μM)	IC ₅₀ Trypo (μM)	CC ₅₀ (μM)
9a	Ph	4-COOHPh	17.95 ± 0.56	138.22 ± 2.82	>>120
9b		Ph	11.81 ± 0.23	68.08 ± 2.95	>>120
9c	4-NO ₂ Ph	Ph	>15	>>100	170.68 ± 4.92
9d	Ph	Ph	10.55 ± 0.21	>>100	>>120
9e	Ph	Bz	>15	>>100	>>120
9f	3,5-di-CH ₃ OPh	Ph	30.52 ± 0.94	>>100	>>120
9g	Ph	4-ClPh	>15	>>100	>>120
9h	Ph	4-CH ₃ -3-NO ₂ Ph	12.59 ± 0.48	27.85 ± 5.60	>>120

appreciable activity against epimastigotes and trypomastigotes. None of the compounds of this series showed cytotoxicity on mammalian cells (Table 3).

From the *Series III*, compounds **13a**, **13b**, **13f**, **13l**, **13m** and **13p** were found to be potent and selective (IC₅₀<10 μM, CC₅₀>100 μM) when tested on the epimastigote form. In contrast, compounds **13c**, **13h-k**, **13o**, **13q** and **13r** displayed high cytotoxicity on Vero cells. We observed that compounds having a 2-chlorobenzyl group in position R1 (**13c** and **13j**) did not exert cytotoxic effects when a methylenedioxy group is located in position R (**13f**). Upon analyzing **13c** and **13p**, which have the same R group, it can be observed that the change of the 2-chlorobenzyl by a benzyl group in R1 abrogates the cytotoxicity. Compounds **13f** y **13p** were found to be the most promising compounds of *Series III* because of their activity against epimastigotes and trypomastigotes, which was similar to that of Bnz (Table 4).

In summary, SAR of this series (I, II, III) demonstrates that the presence of phenacyl group at 1- position in the quinazolinone scaffold; the introduction of aryl or substituted aryl moiety in the quinazolinone core, and the addition of a variety of aryl moieties with donor groups and aminobenzyl group at 2- and 4- positions, respectively, in the quinazolinone ring are essential for the trypanocidal activity.

Out of the three series of compounds analyzed, the derivatives **5a**, **5b**, **9b**, **9h**, **13f** and **13p** were the most active to kill the parasite (epimastigotes and trypomastigotes) while being non-cytotoxic for mammalian cells.

3.3. Computational Chemistry

3.3.1 Quantitative-structure Activity Relationship

Quantitative structure-activity relationship (QSAR) studies play essential roles in pharmaceutical research to identify and generate high-quality leads in the early stages of drug discovery. QSAR studies help reduce the costly failures of

drug candidates by identifying promising lead compounds and reducing the number of costly experiments. As long as the promising results obtained in the biological assays performed with these three chemically diverse collections, prompted us to find the relationship between the chemical features of our derivatives and the observed anti-*T. cruzi* activity. To this end, we decided to conduct a classical QSAR multiple linear regression (MLR) study by considering the logarithmic IC₅₀ values of our compounds as the dependent variable, and calculated *ca.*14444 descriptors which included constitutional, topological, geometrical, 2D autocorrelation, and electrotopological classes to serve as independent variables. The best model capable of describing the inhibitory pattern against both epimastigotes and trypomastigotes is illustrated by the following equations (Equation 1 and Equation 2):

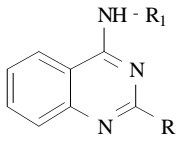
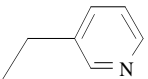
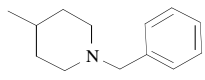
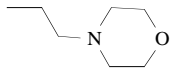
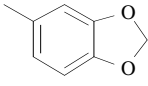
Equation 1

$$pI_{50}Epi(\text{predicted}) = -0.4746(0.1781).A\text{Log}p2 + 4.2959(0.0375).FMF + 2.381(0.0206).VR3_D + 2.3769$$

$$n: 25, R^2: 0.595, Q^2_{LOOCV}: 0.543, F: 33.7, p < 0.0001$$

The FMF descriptor is an approach to characterizing molecular complexity based on the Murcko framework present in the molecule. The descriptor is the ratio of heavy atoms in the framework to the total number of heavy atoms in the molecule. It has been demonstrated that the FMF correlates to the ADMET properties, such as solubility, permeability and cytochrome P450 isoform 3A4 inhibition. The VR3_D descriptor is the logarithmic Randic-like eigenvector-based index from topological distance matrix. The above MLR model gave a moderate Pearson correlation squared coefficient of 0.595 (RMSD=0.122). The model predictability gave a Q²_{LOOCV} value of 0.543.

Table 4. *In vitro* anti-trypansomal activity and cytotoxicity of 2,4-disubstituted-quinazoline derivatives.

Series III					
Cmpd.	R	R ₁	IC ₅₀ Epi (μM)	IC ₅₀ Trypo (μM)	CC ₅₀ (μM)
13a	Ph		7.43 ± 0.8	>>100	111.54 ± 5.24
13b	Ph	Bz	2.75 ± 0.48	50.64 ± 2.80	108.35 ± 2.75
13c	4-CH ₃ OPh	2-ClBz	14.04 ± 0.56	22.88 ± 2.15	18.58 ± 4.45
13d	Ph		>15	127.31 ± 3.66	75.84 ± 3.20
13e	Ph		>15	>>100	81.21 ± 5.77
13f		2-ClBz	3.04 ± 0.75	56.15 ± 5.72	>>120
13g	Ph	2-EtCOOPh	>15	287.28 ± 4.05	75.80 ± 4.77
13h	Ph	2-CH ₃ Ph	10.57 ± 0.67	408.31 ± 4.25	14.81 ± 2.88
13i	Ph	Ph	6.38 ± 0.39	>>100	38.42 ± 5.65
13j	Ph	2-ClBz	5.80 ± 0.27	>>100	25.30 ± 4.27
13k	Ph	4-FBz	8.00 ± 0.43	507.10 ± 7.55	32.53 ± 4.80
13l	Ph	4-CH ₃ OBz	9.86 ± 0.52	40.70 ± 3.77	129.22 ± 3.22
13m	Ph	2-CH ₃ Bz	9.98 ± 0.37	409.39 ± 7.52	> 120
13n	Ph	4-CH ₃ Bz	28.27 ± 0.60	527.2 ± 4.85	34.07 ± 3.20
13o	Ph	3-CF ₃ Ph	13.01 ± 0.38	ND	< 3
13p	4-CH ₃ OPh	Bz	7.79 ± 0.20	35.45 ± 3.20	>>120
13q	Ph	4-CH ₃ OPh	7.71 ± 0.09	ND	<3
13r	Ph	4-ClBz	5.63 ± 0.45	ND	<3

Equation 2

$$pI_{50Tryo(predicted)} = -2.5429(0.1093).GATS1c - 0.5941(0.1707).C1SP3 + 2.9570(0.0764).topoShape + 5.4765$$

$$n: 18 \quad R^2: 0.626, \quad Q^2_{LOOCV}: 0.573, \quad F: 26.7, \quad p < 0.0001$$

The descriptors found for this equation where the Geary autocorrelation -lag 1 / weighted by atomic charges (GATS1c), the index of molecular connectivity to carbon atom, in terms of hybridization (C1SP3) the topoShape descriptor, which is a measure of the molecular anisotropy. The above MLR model gave a moderate R^2 value of 0.626 (RMSD = 0.256). The model predictability gave a Q^2_{LOOCV} value of 0.573.

In order to obtain a better predicting biological activities model, we extended the classic MLR methodology with a back-propagation neural network analysis (BNN) approach (utilizing LOOCV). The artificial neural network analysis (ANN) is one of the most widely used methods for developing non-linear models. The BNN developed herein comprised three layers: the input, hidden, and output layers (4, 4, 1) and the rest of the settings were by default. This BNN was used as a feature mapping method to construct the non-linear model.

Epimastigote activity: Training set (TS) selected with a 75% splitting stratified sampling of the complete set of compounds with active/inactive classification (25 structures). The relevant descriptors found with this approach were the mean topological charge index of order 3 (JGI3), the centred Broto-Moreau autocorrelation of lag 6 weighted by atomic

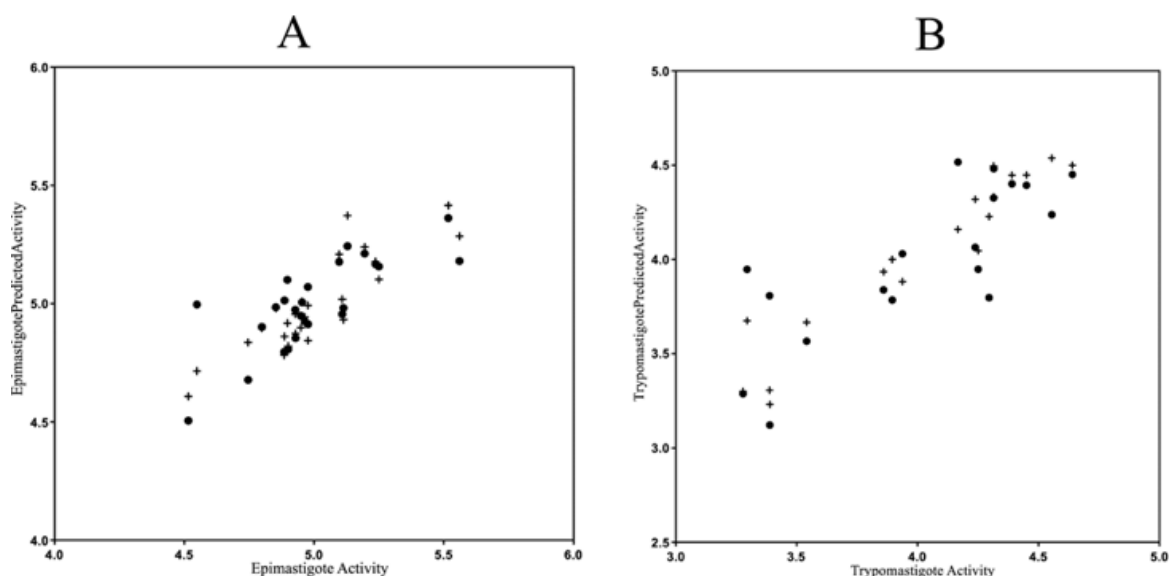


Fig. (3). Comparative outcome for both, MLR and ANN QSAR model strategies for Epimastigote (A) and Trypomastigote (B) activity. Dots = MLR-QSAR model. Crosses = ANN-QSAR model.

Table 5. Calculated pharmacological characteristics, experimental solubility and stability for active compounds.

Cmpd.	IC ₅₀ EPI (μM) ^a	QlogP ^b	QlogS ^c	QPCaco ^d	#met ^e	Aqueous Solubility ^f μg/mL			PBS Stability (h)
						pH 2.0	pH 6.5	pH 7.4	
5a	15.89	3.34	-3.38	1369	2	4.60	3.90	3.00	>48
5b	12.68	3.84	-3.61	1371	2	5.30	3.80	4.20	>48
9b	11.81	5.10	-5.80	6736	1	29.11	5.34	1.19	>48
9h	12.59	3.51	-5.10	820	5	42.40	4.01	3.65	>48
13f	3.04	2.57	-4.25	503	4	166.50	3.28	1.10	>48
13p	7.79	5.21	-5.73	6766	2	137.60	4.10	2.82	>48

^aIC₅₀ (μM) was calculated from dose–response curves by the Prism software. Results represent the average of two or more independent experiments.

^boctanol/water partition coefficient (log Po/w)

^caqueous solubility

^dCaco-2 cell permeability

^enumber of metabolites

^fExperimental solubility at pH 2, 6.4, 7.4. Reference values at pH 6.4: piroxicam, 7.3 μg/mL; efavirenz, 68.3 μg/mL. Values are expressed as means of two independent experiments, each run in triplicate.

volume (ATSC6v) and the FMF descriptor explained above. The above ANN model gave a moderate R^2 value of 0.626 (RMSD= 0.256). The model predictability gave a Q^2_{LOOCV} value of 0.573 (Fig. 3 A).

Trypomastigote form: TS selected with a 80% splitting stratified sampling of the complete set of compounds with active/inactive classification (24 structures). The descriptors found for this equation where the Geary autocorrelation -lag 1 / weighted by atomic charges (GATS1c), the index of molecular connectivity to carbon atom, in terms of hybridization (C1SP3) and the FMF descriptor. The above ANN model gave a very good R^2 value of 0.910 (RMSD = 0.135). The model predictability gave a Q^2_{LOOCV} value of 0.762 (Fig. 3 B).

In summary, the classical QSAR studies performed provided the understanding of the properties that most influ-

enced the anti-*T. cruzi* activity of quinazolinone and quinazoline derivatives. Comparison between statistical parameters of ANN and MLR models in epimastigote and trypomastigote form indicates that the ANN model produces better predicted model. The findings suggested that topological complexity and electrotopological properties are the most crucial molecular features for the anti-*T. cruzi* activity.

3.4. Physicochemical Predictions and Aqueous Solubility of the Selected Compounds

The pharmacological characteristics of drug candidates were predicted with the *QikProp* software [36] summarized in Table 5. *QikProp* generates physically relevant descriptors and uses them to perform ADMET predictions. A compound is viewed as potentially problematic if it does not satisfy a “rule-of-three”: predicted log $S > -6.0$, $P_{Caco} > 30$ nm/s, and

maximum number of primary metabolites of six. The most potent compounds reported herein comply with all these limits (Table 5).

We next tested the *in vitro* solubility and stability in PBS of the top six compounds. In humans, the stomach pH value is 1.0-2.0, while in the small intestine, pH values are 5.0-7.0. Because compound solubility often depends on solution pH, it is important to consider different pH buffers. Taking into account the relevance of drug solubility in *in vivo* absorption and distribution, we chose pH values of 2.0, 6.4, and 7.4 for the analysis.

Solubility data are summarized in Table 5. Compounds **9b**, **9h**, **13f**, **13p** presented considerable solubility values under acidic conditions (29.11-166.50 µg/mL), which ensures good absorbability in the stomach. A comparison of the compounds **9h**, **9b** (*Series II*) and **13 f**, **13p** (*Series III*) showed that the compounds belonging to *series III* are more soluble at pH 2.0 than those belonging to *series II*. The latter phenomenon might probably be due to the presence of the free amino group. Compounds **5a**, **5b** had poor solubility at the different pH evaluated. The aqueous solubility pattern of the assayed compounds was similar to the predicted solubility. All the compounds also had a reasonable stability in PBS (>48 h), so no intrinsic chemical stability issues were expected.

CONCLUSION

Quinazolinone and quinazoline derivatives represent an interesting new family of drugs to control the multiplication of *T. cruzi* within the host cell. Six compounds (**5a**, **5b**, **9b**, **9h**, **13f** and **13p**) showed a low micromolar activity against the epimastigote and trypomastigote forms with desirable drug-like properties. A QSAR study was carried out to find the relationship between the physicochemical parameters of quinazoline and quinazolinone derivatives and their anti-*T. cruzi* activity. This study indicated that topological complexity and electrotopological properties are crucial molecular features for the biological activity observed.

The results obtained herein give new insights to improve the anti-*T. cruzi* activity of quinazoline and quinazolinone derivatives and could help to develop new antichagasic compounds.

ETHICS APPROVAL AND CONSENT TO PARTICIPATE

Not applicable.

HUMAN AND ANIMAL RIGHTS

No Animals/Humans were used for studies that are the basis of this research.

CONSENT FOR PUBLICATION

Not applicable.

CONFLICT OF INTEREST

The authors declare no conflict of interest, financial or otherwise.

ACKNOWLEDGEMENTS

This work was supported by grants from Universidad de Buenos Aires, Argentina (UBACYT 2014-2017 200201301 00449BA and UBACYT 2016 Mod I 20020150100130BA to AMB), UBACYT 20020100100521, to EL), Agencia Nacional de Promoción Científica y Tecnológica, Argentina (PICT 2014-1884 to MB), CONICET (PIP 2014 11220 130100721 to MB). Authors thank the TUPAC Cluster from CSC-CONICET, which is part of SNCAD-MinCyT, Argentina. Authors wish to thank Dr. Mariela Videla for her technical assistance and use of mass spectrometry facility at CI-BION and Lourdes M. Penayo Paiz for her technical assistance with the organic synthesis.

SUPPLEMENTARY MATERIAL

Supplementary data associated with this article contains methods and ¹H-RMN and ¹³C-RMN spectra of all the compounds.

REFERENCES

- [1] W.H.O. <http://www.who.int/mediacentre/factsheets/fs340/en/> Accessed December 20, 2017
- [2] Nunes, M.C.P.; Dones, W.; Morillo, C.A.; Encina, J.J.; Ribeiro, A.L. Chagas disease: An overview of clinical and epidemiological aspects. *J. Am. Coll. Cardiol.*, **2013**, *62*, 767-776.
- [3] Castro, J.; Montalto de Mecca, M.; Bartel, L. Toxic side effects of drugs used to treat Chagas' disease (American trypanosomiasis). *Hum. Exp. Toxicol.*, **2006**, *25*, 471-479.
- [4] Andrews, K.T.; Fisher, G.; Skinner-Adams, T.S. Drug repurposing and human parasitic protozoan diseases. *Int. J. Parasitol.: Drugs Drug Resist.*, **2014**, *4*, 495-1111.
- [5] Al-Salem, H.S.A.; Hegazy, G.H.; El-Taher, K.E.H.; El-Messery, S.M.; Al-Obaid, A.M.; El-Subbagh, H.I. Synthesis, anticonvulsant activity and molecular modeling study of some new hydrazinecarbothioamide, benzenesulfonohydrazide, and phenacylaceto-hydrazide analogues of 4(3H)-quinazolinone. *Bioorg. Med. Chem. Lett.*, **2015**, *25*, 1490-1499.
- [6] Wang, X.; Xin, M.; Xu, J.; Kang, B.; Li, Y.; Lu, S.; Zhang, S. Synthesis and antitumor activities evaluation of m - (4- morpholinoquinazolin-2-yl) benzamides in vitro and in vivo. *Eur. J. Med. Chem.*, **2015**, *96*, 382-395.
- [7] Vani, K.V.; Ramesh, G.; Rao, C.V. Synthesis of New Triazole and Oxadiazole Derivatives of Quinazolin-4(3H)-one and Their Antimicrobial Activity. *Heterocyclic Chem.*, **2016**, *53*, 719-726.
- [8] Gobinath, M.; Subramanian, N.; Alagarsamy, V. Design, synthesis and H1-antihistaminic activity of novel 1-substituted-4-(3-chlorophenyl)-[1,2,4]triazolo[4,3-a]quinazolin-5(4H)-ones. *J. Saudi Chem. Soc.*, **2015**, *19*, 282-286.
- [9] Hu, J.; Zhang, Y.; Dong, L.; Wang, Z.; Chen, L.; Liang, D.; Shi, D.; Shan, X.; Liang, G. Design, Synthesis and Biological Evaluation of Novel Quinazoline Derivatives as Anti-inflammatory Agents against Lipopolysaccharide-induced Acute Lung Injury in Rats. *Chem. Biol. Drug Des.*, **2015**, *85*, 672-684.
- [10] Gilson, P.R.; Tan, C.; Jarman, K.E.; Lowes, K.N.; Curtis, J.M.; Nguyen, W.; Di Rago, A.E.; Bullen, H.E.; Prinz, B.; Duffy, S.; Baell, J.B.; Hutton, C.A.; Subroux, H.J.; Crabb, B.S.; Avery, V.M.; Cowman, A.F.; Sleebs, B.E. Optimization of 2-Anilino 4-Amino Substituted Quinazolines into Potent Antimalarial Agents with Oral in Vivo Activity. *J. Med. Chem.*, **2017**, *60*, 1171-1188.
- [11] Singh, M.; Raghav, N. 2,3-Dihydroquinazolin-4(1H)-one derivatives as potential non-peptidyl inhibitors of cathepsins B and H. *Bioorg. Chem.*, **2015**, *59*, 12-22.
- [12] Wei, M.; Chai, W.M.; Wang, R.; Yang, Q.; Deng, Z.; Peng, Y. Quinazolinone derivatives: Synthesis and comparison of inhibitory mechanisms on α -glucosidase. *Bioorganic Med. Chem.*, **2017**, *25*, 1303-1308.
- [13] Cavalli, A.; Lizzi, F.; Bongarzone, S.; Brun, R.; Luise Krauth-Siegel R.; Bolognesi, M.L. Privileged structure-guided synthesis of

- quinazoline derivatives as inhibitors of trypanothione reductasa. *Bioorganic Med. Chem. Lett.*, **2009**, *19*, 3031–3035.
- [14] Mendoza-Martínez, C.; Correa-Basurto, J.; Nieto-Meneses, R.; Márquez-Navarro, A.; Aguilar-Suárez, R.; Montero-Cortes, M.D.; Nogueira-Torres, B.; Suárez-Contreras, E.; Galindo-Sevilla, N.; Rojas-Rojas, Á.; Rodríguez-Lezama, A.; Hernández-Luis, F. Design, synthesis and biological evaluation of quinazoline derivatives as anti-trypanosomatid and anti-plasmodial agents. *Eur. J. Med. Chem.* **2015**, *96*, 296–307.
- [15] Khatib, T.K.; El-Bayouki, K.A.M.; Basyouni, W.M.; El-basyoni, F.A.; Ali, M.M.; Abbas, S.Y.; Mostafa, E.A. Sulfamic Acid as an Efficient, Cost-Effective, Eco-Friendly and Recyclable Solid Acid Catalyst for the Synthesis of a Novel Series of 2,3-Dihydroquinazolin-4(1H)-ones and Antitumor Evaluation. *Research Journal of Pharmaceutical, Biological and Chemical Sciences*, **2015**, *6*, 281–291.
- [16] Esteva, M.; Ruiz, A.M.; Stoka, A.M. Trypanosoma cruzi: methoprene is a potent agent to sterilize blood infected with tripomastigotes. *Exp. Parasitol.*, **2002**, *100*, 248–251.
- [17] Frank, M.F.; Cicarelli, A.B.; Bollini, M.; Bruno, A.M.; Batlle, A.; Lombardo, M.E. Trypanocidal activity of thioamide-substituted imidazoquinolinone: Electrochemical properties and biological effects. *Evidence-based Complement. Altern. Med.*, **2013**, *2013*, 1–10. Article ID 945953.
- [18] Jorgensen WL, n.d. QikProp, v 3.0; Schrödinger LLC.
- [19] Yap, C.W. PaDEL-descriptor: An open source software to calculate molecular descriptors and fingerprints. *J. Comput. Chem.*, **2011**, *32*, 1466–1474.
- [20] Meinl, T.; Jagla, B.; Berthold, M.R. Integrated data analysis with KNIME, Published by Woodhead Publishing Limited, **2012**.
- [21] Hall, M.; Frank, E.; Holmes, G.; Pfahringer B.; Reutemann, P.; Witten, I.H. The WEKA data mining software, SIGKDD. *Explor. Newsl.*, **2009**, *11*, 10–18.
- [22] Palacios-Bejarano, B.; Cerruela García, G.; Luque Ruiz, I.; Gómez-Nieto, M.A. QSAR model based on weighted MCS trees approach for the representation of molecule data sets. *J. Comput. Aided Mol. Des.*, **2013**, *27*, 185–201.
- [23] Sochacka, J. Docking of thiopurine derivatives to human serum albumin and binding site analysis with Molegro Virtual Docker. *Acta Pol. Pharm.*, **2014**, *71*, 343–349.
- [24] Venkatraman, V.; Dalby, A.R.; Yang, Z.R. Evaluation of Mutual Information, Genetic Algorithm and SVR for Feature Selection in QSAR Regression. *J. Chem. Inf. Comput. Sci.*, **2004**, *44*, 1688–1692.
- [25] Tropsha, A.; Gramatica, P.; Gombar, V. The Importance of Being Earnest: Validation is the Absolute Essential for Successful Application and Interpretation of QSPR Models. *QSAR Comb. Sci.*, **2003**, *22*, 69–77.
- [26] Baskin, I.I.; Winkler, D.I.; Tetko, V. A renaissance of neural networks in drug discovery. *Expert Opin. Drug Discov.*, **2016**, *11*, 785–795.
- [27] Leal, E.S.; Aucar, M.G.; Gebhard, L.G.; Iglesias, N.G.; Pascual, M.J.; Casal, J.J.; Gamarnik, A.V.; Cavasotto, C.N.; Bollini, M. Discovery of novel dengue virus entry inhibitors via a structure-based approach. *Bioorg. Med. Chem. Lett.*, **2017**, *27*, 3851–3855.
- [28] Shestakov, A.S.; Sidorenko, O.E.; Bushmarinov, I.S.; Shikhaliev, K.S.; Antipin, M.Y. 3-aryl(alkyl)quinazoline-2,4(1H,3H)-diones and their alkyl derivatives. *Russ. J. Org. Chem.*, **2009**, *45*, 1691–1696.
- [29] Leticia Guerrero, R.; Rivero, I.A. Reaction of o-aminobenzamides with dialkyl carbonates and ionic liquids: A novel one-pot, high-yield, microwave-assisted synthesis of 1-alkylquinazoline-2,4-diones. *J. Mex. Chem. Soc.*, **2012**, *56*, 201–206.
- [30] Cortez, R.; Rivero, I.; Somanathan, R.; Aguirre, G.; Ramirez, F.; Hong, E. Synthesis of Quinazolinone Using Triphosgene. *Synth. Commun.*, **1991**, *21*(2), 285–292.
- [31] Petrov, J.S.; Andreev, G.N. Synthesis of 2,4 (1H,3H)-Quinazolinone and 3-substituted 2,4 (1H,3H)-Quinazolinones. *Org. Prep. Proced. Int.*, **2005**, *37*, 560–565.
- [32] Abbas, S.Y.; El-Bayouki, K.A.M.; Basyouni, W.M. Utilization of isatoic anhydride in the syntheses of various types of quinazoline and quinazolinone derivatives. *Synth. Commun.*, **2016**, *46*, 993–1035.
- [33] Alinezhad, H.; Tajbakhsh, M.; Ghobadi, N. Synthesis of 2, 3-dihydroquinazolin-4 (1H)-ones using Bronsted acidic ionic liquid. *Research and Reviews in Material Sciences and Chemistry*, **2014**, *3*(2), 123–135.
- [34] Chawla A.; Batra, C. Recent advances of quinazolinone derivatives as marker for various biological activities. *Int. Res. J. Pharm.*, **2013**, *4*, 49–58.
- [35] Cheng, R.; Guo, T.; Zhang-Negrerie, D.; Du, Y.; Zhao, K. One-Pot Synthesis of Quinazolinones from Anthranilamides and Aldehydes via *p*-Toluenesulfonic Acid Catalyzed Cyclocondensation and Phenylodine Diacetate Mediated Oxidative Dehydrogenation. *Synthesis*, **2013**, *45*(21), 2998–3006.
- [36] Jorgensen, W.L.; Duffy, E.M. Prediction of drug solubility from structure. *Adv. Drug Deliv. Rev.*, **2002**, *54*, 355–366.